Check for updates

STRUCTURAL CHEMISTRY

ISSN 2053-2296

Crystallographic evidence for unintended benzisothiazolinone 1-oxide formation from benzothiazinones through oxidation

Tamira Eckhardt,[a] Richard Goddard,[b] Christoph Lehmann,[a] Adrian Richter,[a] Henok Asfaw Sahile,[c] Rui Liu,[d] Rohit Tiwari,[d] Allen G. Oliver,[d] Marvin J. Miller,[d] Rüdiger W. Seidel[a]* and Peter Imming[a]

[a]Institut für Pharmazie, Martin-Luther-Universität Halle-Wittenberg, Wolfgang-Langenbeck-Strasse 4, 06120 Halle (Saale), Germany, [b]Max-Planck-Institut für Kohlenforschung, Kaiser-Wilhelm-Platz 1, 45470 Mülheim an der Ruhr, Germany, [c]Department of Medicine and Department of Microbiology and Immunology, University of British Columbia, Vancouver, British Columbia, V6T 1Z3, Canada, and [d]Department of Chemistry and Biochemistry, University of Notre Dame, Indiana 46556, USA. *Correspondence e-mail: ruediger.seidel@pharmazie.uni-halle.de

Received 29 June 2020
Accepted 9 August 2020

Edited by M. Gardiner, Australian National University, Australia

Keywords: benzothiazinone; BTZ043; benziso-thiazolinone; ring contraction; crystal structure; antimycobacterial activity.

CCDC references: 2022514; 2022515

Supporting information: this article has supporting information at journals.iucr.org/c

1,3-Benzothiazin-4-ones (BTZs) are a promising new class of drugs with activity against *Mycobacterium tuberculosis*, which have already reached clinical trials. A product obtained in low yield upon treatment of 8-nitro-2-(piperidin-1-yl)-6-(trifluoromethyl)-4*H*-benzothiazin-4-one with 3-chloroperbenzoic acid, in analogy to a literature report describing the formation of sulfoxide and sulfone derived from BTZ043 [Tiwari *et al.* (2015). *ACS Med. Chem. Lett.* **6**, 128–133], is a ring-contracted benzisothiazolinone (BIT) 1-oxide, namely, 7-nitro-2-(piperidine-1-carbonyl)-5-(trifluoromethyl)benzo[*d*]isothiazol-3(2*H*)-one 1-oxide, $C_{14}H_{12}F_3N_3O_5S$, as revealed by X-ray crystallography. Single-crystal X-ray analysis of the oxidation product originally assigned as BTZ043 sulfone provides clear evidence that the structure of the purported BTZ043 sulfone is likewise the corresponding BIT 1-oxide, namely, 2-[(*S*)-2-methyl-1,4-dioxa-8-azaspiro[4.5]-decane-8-carbonyl]-7-nitro-5-(trifluoromethyl)benzo[*d*]isothiazol-3(2*H*)-one 1-oxide, $C_{17}H_{16}F_3N_3O_7S$. A possible mechanism for the ring contraction affording the BIT 1-oxides instead of the anticipated constitutionally isomeric BTZ sulfones and antimycobacterial activities thereof are discussed.

1. Introduction

Due to extremely low cidal concentrations against *Mycobacterium tuberculosis in vitro*, 8-nitro-1,3-benzothiazin-4-ones (BTZs) have been the focus of many chemical, pharmacological and, recently, clinical studies (Mikušová *et al.*, 2014; Kloss *et al.*, 2017; Makarov & Mikušová, 2020). Several promising compounds with improved aqueous solubilities have been identified with potent antitubercular activity (Zhang *et al.*, 2019). The first small molecule crystal structure of a BTZ, namely macozinone (PBTZ169), was reported in this journal by Zhang & Aldrich (2019). So far, the excellent *in vitro* activity appears not to translate to the low daily doses aspired for a medication that needs to be administered for months (Lupien *et al.*, 2018). This could be attributed to pharmacokinetic problems and rapid metabolism by gut bacteria (Lv *et al.*, 2017).

Research interest in this compound class is also inspired by the chemical versatility of the BTZs, which offer several points of attack, especially for nucleophiles and reducing agents (Tiwari *et al.*, 2013). In turn, the BTZ S atom appears to be not very susceptible to oxidation. When BTZ043 (Scheme 1) was treated with the oxidizing agent 3-chloroperbenzoic acid at room temperature for several days, a major amount of

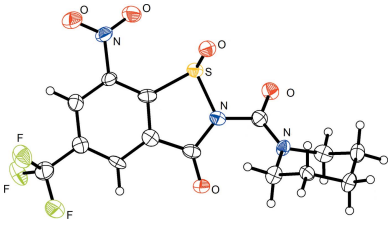

OPEN ACCESS

unreacted BTZ starting material was recovered and small quantities of two oxidation products were isolated. Based on ^{1}H NMR spectroscopy and the sum formula calculated from high-resolution mass spectrometry, the corresponding BTZ sulfoxide and sulfone structures were assigned (Tiwari *et al.*, 2015).

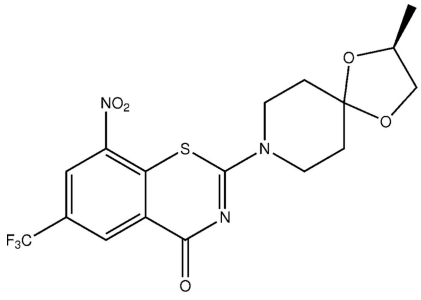

BTZ043

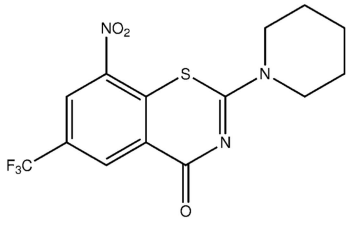

1

Scheme 1

Treatment of 8-nitro-2-(piperidin-1-yl)-6-(trifluoromethyl)-4*H*-benzothiazin-4-one (**1**, Scheme 1) with 3-chloroperbenzoic acid in a similar way and crystallographic characterization of one of the oxidation products revealed the formation of a ring-contracted benzisothiazolone (BIT) 1-oxide instead of the anticipated BTZ sulfone (Fig. 1). Subsequent crystallographic reinvestigation of the BTZ043 oxidation product originally described as BTZ sulfone by us (Tiwari *et al.*, 2015) evidenced that the structure must be revised to the corresponding ring-contracted BIT 1-oxide. In this article, we report the structural characterization of BIT 1-oxides resulting from oxidation of **1** and BTZ043, and propose a reaction mechanism of the ring contraction. We furthermore show by analysis of spectroscopic data and deliberate synthesis that the purported BTZ sulfoxide is actually a BIT.

2. Experimental

2.1. General

Starting materials were obtained from commercial sources and were used as received. Solvents were of analytical grade. Compound **1** was synthesized as described elsewhere (Rudolph *et al.*, 2016). Thin-layer chromatography (TLC) was performed on Silica gel 60 F_{254} TLC plates (Merck KGaA, Darmstadt). The reported R_F values are uncorrected. Flash chromatography was carried out with a 40 g puriFlash column (30 µm silica gel, 60 Å, 500 $m^2\,g^{-1}$, Interchim, Montluçon, France). Preparative HPLC was performed on a Shimadzu LC-10AD system using 19 × 150 mm XTerra RP-18 columns (7 µm, Waters, Milford, Massachusetts, USA). ^{1}H and ^{13}C NMR spectra were recorded at room temperature on an Agilent Technologies VNMRS 400 MHz NMR spectrometer (*bs* = broad singlet, *q* = quartet and *m* = multiplet). Chemical shifts are referenced to the residual signals of $CDCl_3$ (δ_H = 7.26 ppm and δ_C = 77.0 ppm). High-resolution mass spectra (HRMS) were measured on a Bruker Daltonics APEXIII FT–ICR mass spectrometer.

2.2. Synthesis and crystallization

Compounds **2** and **3** were obtained when **1** was treated with 3-chloroperbenzoic acid, adapting the procedure described by Tiwari *et al.* (2015). A solution of 3-chloroperbenzoic acid (1.04 g, 6.0 mmol) in dichloromethane (6.5 ml) was added dropwise to a stirred solution of 8-nitro-2-(piperidin-1-yl)-6-(trifluoromethyl)-4*H*-1,3-benzothiazin-4-one, **1** (1.09 g, 3.0 mmol), in dichloromethane (5 ml) at 0 °C. After stirring for 4 d at room temperature, additional 3-chloroperbenzoic acid (0.5 g) was added and the mixture was stirred for another day. The resulting mixture was washed twice with a saturated sodium bicarbonate solution (55 ml) and then once with deionized water (55 ml). After drying over sodium sulfate, the solvent was removed using a rotary evaporator. The crude product was subjected to flash chromatography [gradient of 50–100 (*v*/*v*) ethyl acetate/heptane] to give **2** and **3**. Both compounds were purified by HPLC [gradient of 5–95 (*v*/*v*) acetonitrile/water in 10 min + 0.05% trifluoroacetic acid] to yield 6 mg of **2** (0.016 mmol, 0.5%) and 35 mg of **3** (0.089 mmol, 3%).

Crystals of **3** suitable for single-crystal X-ray analysis were obtained after a couple of days when a solution of *ca* 5 mg of the compound in ethanol (1.5 ml) in a 10 × 50 mm glass vial with a screw cap was left at room temperature and the solvent allowed to evaporate slowly.

The synthesis of **4** has been reported elsewhere (Tiwari *et al.*, 2015; therein mistaken for the sulfone of the BTZ043 starting material). For the preparation of crystals suitable for single-crystal X-ray analysis, the compound (1 mg) was added

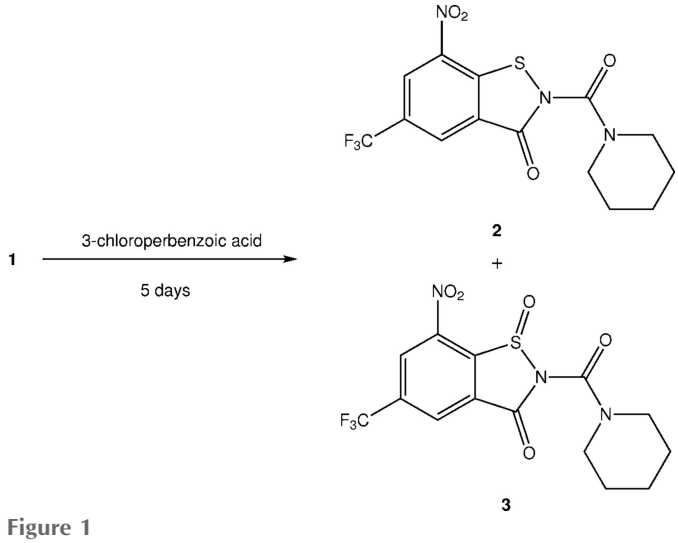

Figure 1
Ring-contracted oxidation products resulting from the treatment of **1** with 3-chloroperbenzoic acid at room temperature.

Table 1
Experimental details.

Experiments were carried out with Cu $K\alpha$ radiation. Refinement in both cases was with 1 restraint. H-atom parameters were constrained.

	3	**4**
Crystal data		
Chemical formula	$C_{14}H_{12}F_3N_3O_5S$	$C_{17}H_{16}F_3N_3O_7S$
M_r	391.33	463.39
Crystal system, space group	Orthorhombic, *Iba*2	Monoclinic, $P2_1$
Temperature (K)	100	120
a, b, c (Å)	17.6719 (8), 25.7296 (12), 6.8887 (3)	8.8165 (2), 16.1649 (4), 13.4246 (3)
α, β, γ (°)	90, 90, 90	90, 90.0022 (12), 90
V (Å^3)	3132.2 (2)	1913.24 (8)
Z	8	4
μ (mm^{-1})	2.50	2.23
Crystal size (mm)	0.23 × 0.06 × 0.04	0.25 × 0.07 × 0.04
Data collection		
Diffractometer	Bruker Kappa Mach3 APEXII	Bruker PHOTON-II
Absorption correction	Gaussian (*SADABS*; Bruker, 2012)	Numerical (*SADABS*; Bruker, 2012)
T_{min}, T_{max}	0.748, 0.936	0.715, 0.949
No. of measured, independent and observed $[I > 2\sigma(I)]$ reflections	22457, 2477, 1843	36857, 7140, 6860
R_{int}	0.102	0.041
$(\sin\theta/\lambda)_{max}$ (Å^{-1})	0.610	0.611
Refinement		
$R[F^2 > 2\sigma(F^2)]$, $wR(F^2)$, S	0.059, 0.170, 1.08	0.033, 0.083, 1.04
No. of reflections	2477	7140
No. of parameters	235	561
$\Delta\rho_{max}$, $\Delta\rho_{min}$ (e Å^{-3})	0.53, −0.75	0.61, −0.31
Absolute structure	Flack x determined using 550 quotients $[(I^+) - (I^-)]/[(I^+) + (I^-)]$ (Parsons *et al.*, 2013)	Flack x determined using 3080 quotients $[(I^+) - (I^-)]/[(I^+) + (I^-)]$ (Parsons *et al.*, 2013)
Absolute structure parameter	0.08 (5)	0.017 (6)

Computer programs: *APEX3* (Bruker, 2015), *SAINT* (Bruker, 2015), *SHELXT* (Sheldrick, 2015*a*), *SHELXL2018* (Sheldrick, 2015*b*), *DIAMOND* (Brandenburg, 2018), *enCIFer* (Allen *et al.*, 2004) and *publCIF* (Westrip, 2010).

to a 6 × 50 mm round-bottomed borosilicate glass culture tube, and dissolved in chloroform (0.4 ml) to give a clear homogenous solution. The tube was placed in a 20 ml scintillation vial, followed by the addition of pentane (5 ml). The vial was capped tightly and the resulting diffusion chamber was allowed to stand undisturbed at room temperature. After several days, crystals suitable for X-ray analysis formed.

2.2.1. Analytical data for 2. ^{1}H NMR (400 MHz, $CDCl_3$): δ 8.77 (*bs*, 1H), 8.57 (*bs*, 1H), 3.58 (*m*, 4H), 1.78–1.70 (*m*, 6H) ppm; HRMS(ESI): calculated for $C_{14}H_{12}F_3N_3O_4S$ $[M + Na]^+$ 398.0398, found 398.0397; R_F = 0.29 (ethyl acetate/heptane, 2:8 *v*/*v*).

2.2.2. Analytical data for 3. ^{1}H NMR (400 MHz, $CDCl_3$) δ 8.79 (*bs*, 1H), 8.58 (*bs*, 1H), 3.68–3.51 (*m*, 4H), 1.81–1.62 (*m*, 6H) ppm; ^{13}C NMR (101 MHz, $CDCl_3$): δ 159.5, 148.3, 144.8, 143.0, 137.8 (*q*, $^2J_{C,F}$ = 35.5 Hz), 132.8, 129.4 (*q*, $^3J_{C,F}$ = 3.6 Hz), 126.6 (*q*, $^3J_{C,F}$ = 3.6 Hz), 121.6 (*q*, $^1J_{C,F}$ = 274.2 Hz), 47.5, 25.8, 24.0 ppm; HRMS(ESI): calculated for $C_{14}H_{12}F_3N_3O_5S$ $[M + H]^+$ 392.0528, found 392.0526; R_F = 0.22 (ethyl acetate/heptane, 2:8 *v*/*v*).

2.3. Refinement

Crystal data, data collection and structure refinement details are summarized in Table 1. H-atom positions were calculated geometrically, with aromatic C—H = 0.95 Å, methyl C—H = 0.98 Å, methylene C—H = 0.99 Å and methine C—H = 1.00 Å, and refined using a riding model, with U_{iso}(H) = 1.2U_{eq}(C) (1.5 for methyl groups). The torsion angles of the methyl groups were initially determined using a circular Fourier search and subsequently refined while maintaining the tetrahedral structure.

3. Results and discussion

3.1. Synthesis and structural identification

When **1** was treated with 3-chloroperbenzoic acid, adapting the procedure for BTZ043 reported by Tiwari *et al.* (2015), likewise a major amount of the BTZ starting material was recovered, but small quantities of oxidation products **2** and **3** could be isolated by chromatography. The corresponding sum formulae were obtained from high-resolution mass spectra, and **3** was subjected to X-ray crystallography. The X-ray analysis umambiguously revealed the BIT 1-oxide structure for **3** instead of the anticipated BTZ sulfone, which would be a constitutional isomer (Fig. 1). Accordingly, and in agreement with the sum formula, we propose the corresponding BIT structure for **2** instead of the anticipated BTZ sulfoxide, which likewise would be a constitutional isomer.

Single-crystal X-ray analysis of the oxidation product of BTZ043 resulting from treatment with 3-chloroperbenzoic acid, which was named 'BTZ-SO_2' by Tiwari *et al.* (2015), provided clear evidence for the formation of the corre-

Table 2
^{1}H NMR shifts (ppm) of the aromatic protons in $CDCl_3$ for **1**–**3**, BTZ043 and its oxidation products.

Data for **1** were taken from Rudolph *et al.* (2016) and data for BTZ043, 'BTZ-SO' and 'BTZ-SO_2' were taken from Tiwari *et al.* (2015).

1	**2**	**3**	BTZ043	'BTZ-SO'	'BTZ-SO_2' (**4**)
9.08	8.77	8.79	9.02	8.78	8.80
8.72	8.57	8.58	8.55	8.59	8.58

sponding BIT 1-oxide **4**, a constitutional isomer of the reported BTZ sulfone (Fig. 2).

Table 2 compares the ^{1}H NMR shifts of the two aromatic protons in **1** and BTZ043 with those of the derived oxidation products. For both **2** and **3**, as well as 'BTZ-SO' and **4**, the signals assigned to the two aromatic protons are upfield shifted compared with the parent BTZs. While assuming the anticipated BTZ sulfoxide and sulfone structures, Tiwari *et al.* (2015) attributed this effect to the influence of the S-atom lone-pair delocalization and the loss of aromaticity due to the nonplanarity of the 1,4-thiazinone rings in the assumed BTZ sulfoxide and sulfone structures. Higher electron density within the encountered BIT nine-membered heterobicyclic system, as compared with the BTZ ten-membered system, however, provides a better explanation for the shielding of the aromatic protons resulting in the observed upfield shifts. For further corroboration, BIT **2**, for which we did not obtain crystals suitable for single-crystal X-ray analysis, was synthesized deliberately from 2-chloro-3-nitro-5-(trifluoromethyl)-nitrobenzamide (see supporting information), following an established procedure for related BITs (Bhakuni *et al.*, 2012). NMR spectroscopic and mass spectrometric data of the product thus obtained agreed with those for **2** resulting from treatment of **1** with 3-chloroperbenzoic acid.

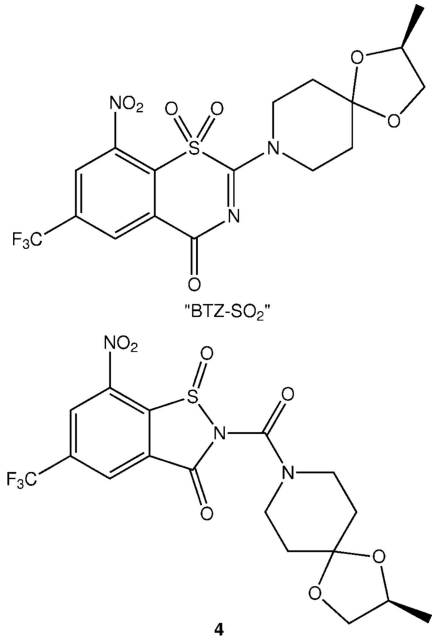

Figure 2
The incorrect structure 'BTZ-SO_2' (Tiwari *et al.*, 2015) and the revised structure of **4**, resulting from treatment of BTZ043 with 3-chloroperbenzoic acid at room temperature.

3.2. Structural descriptions of 3 and 4

Compound **3** crystallizes in the polar orthorhombic space group *Iba*2 with one molecule in the asymmetric unit (Z' = 1). Fig. 3 shows the molecular structure in the crystal. The BIT system is not entirely planar. Atoms N2 and O2 are displaced by 0.27 (1) and −0.20 (1) Å, respectively, above and below the mean plane defined by the benzene ring. The plane of the nitro group is tilted out of this plane by 12 (1)°. The sulfinamide moiety exhibits a pyramidal structure at the S atom, as expected. The molecule in the chosen asymmetric unit is *R*-configured at the S atom. It is worth emphasizing, however, that the *S* enantiomer is generated by glide symmetry in the polar crystal structure so the crystal is a racemate. The central carbamide moiety is tilted out of the BIT plane, as revealed by the torsion angles about the N2—C9 bond. The structure at atom N2 is slightly pyramidal, whereas that at N4 is virtually planar due to conjugation with the adjacent carbonyl group. The piperidine ring adopts a low-energy chair conformation with some deviations of the bond angles from ideal tetrahedal angles, which can be attributed to the planarity at N4.

Compound **4** crystallizes in the Sohncke space group $P2_1$ with two diastereomers in the asymmetric unit (Z' = 2). Fig. 4 depicts displacement ellipsoid plots for both unique molecules. Compared with **3**, compound **4** exhibits an additional spiro-(2*S*)-methyl-1,3-dioxolane group appended to the piperidine ring in the 4-position. The *S* configuration at C15, as in the BTZ043 starting material, is encountered in both crystallographically distinct molecules and the configurational assignment was confirmed by a Flack *x* parameter (Parsons *et al.*, 2013) close to zero with a reasonably small standard uncertainty (Table 1). The two independent molecules exhibit opposite configurations at the S atoms and thus the crystal is a cocrystal of two diastereomers. Possible causes of Z' > 1 crystallization have been discussed (Steed & Steed, 2015). Here, Z' = 2 is attributed to diasteromeric crystallization. The formation of a diastereomeric conglomerate or a solid solution

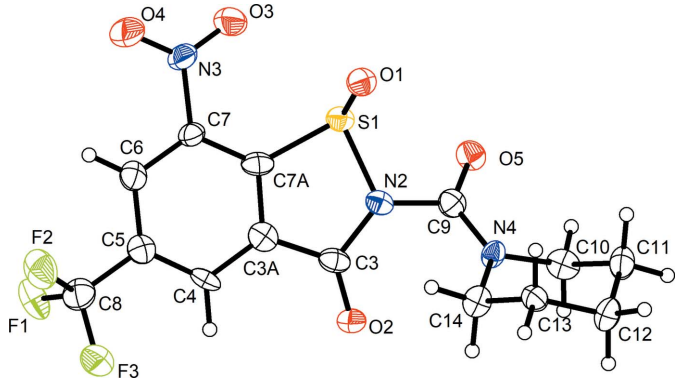

Figure 3
The molecular structure of **3** in the crystal. Displacement ellipsoids are drawn at the 50% probability level. H atoms are represented by small spheres of arbitrary radii.

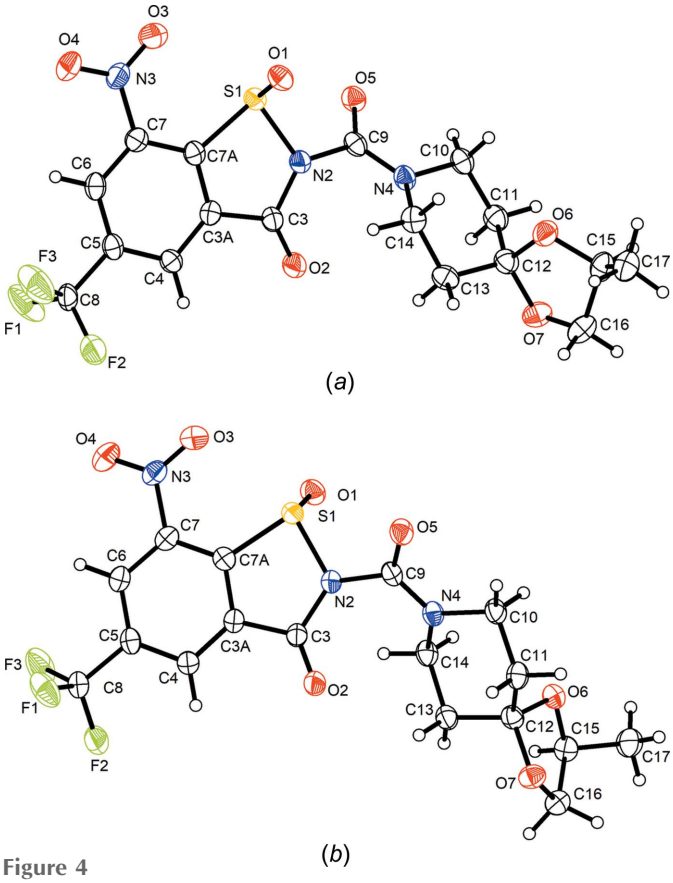

Figure 4
Displacement ellipsoid plots (50% probability level) of the two crystallographically distinct diastereomeric molecules of **4**. H atoms are represented by small spheres of arbitrary radii.

would have been an alternative crystallization pathway. Apart from the configuration at the S atom, the distinct molecules also exhibit different conformations of the 1,3-dioxolane five-membered rings. In molecule 1 (Fig. 4*a*), the 1,3-dioxolane ring adopts an envelope conformation with atom C16 on the flap, whereas in molecule 2 (Fig. 4*b*), the ring is close to an envelope with the spiro atom C12 on the flap. As in **3**, the BIT systems deviate slightly from planarity. In molecule 1, atom O2 is displaced from the mean plane of the benzene ring by 0.323 (6) Å, and in molecule 2, atoms N2 and O2 deviate by −0.118 (5) and 0.333 (5) Å, respectively, from this plane. The tilt angle between the mean plane of the benzene ring and the plane of the nitro group is 16.4 (3)° in molecule 1 and 10.7 (4)° in molecule 2. Similar to **3**, in both molecules, the central carbamide moiety is tilted out of the plane of the BIT skeleton and the appended piperidine ring adopts a low-energy chair conformation with some minor deviations of the bond angles.

The supramolecular structure of **4** in the solid state features short C—F···F—C contacts [F1_1···F3_2^{i} = 2.737 (4) Å and F3_1···F1_2^{ii} = 2.751 (4) Å)], which link unique molecules 1 and 2 along the [100] direction (Fig. 5). According to the corresponding C—F···F angles in the range of 157.8–167.8°, these contacts may be classified as type-I F··· F interactions (Baker *et al.*, 2012). F···F contacts that are shorter than the sum of the van der Waals radii are not encountered in the crystal structure of **3**, but instead several short C—H···F contacts are observed (not depicted).

3.3. Mechanistic discussion of the ring contraction

Since the ring-contracted oxidation products only formed in very low yields, investigation of the reaction mechanism of BTZ oxidation and rearrangement upon treatment with 3-chloroperbenzoic acid was not undertaken. We propose the sequence shown in Fig. 6. This is in part based on a mechanism

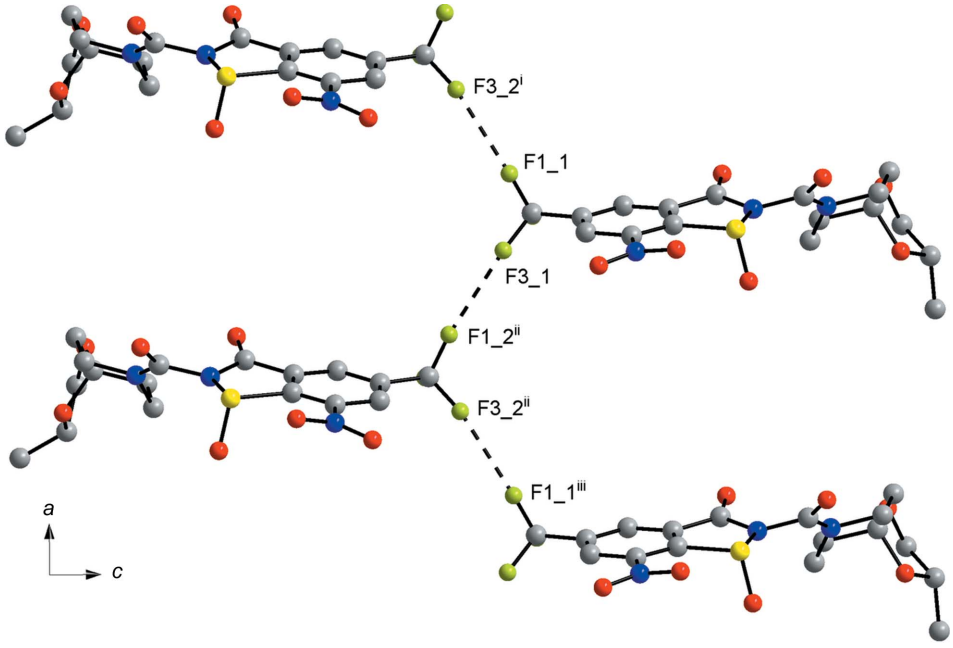

Figure 5
Part of the crystal structure of **4**, showing C—F···F—C contacts (dashed lines), viewed down the *b*-axis direction towards the origin. [Symmetry codes: (i) *x*, *y*, *z* − 1; (ii) *x* − 1, *y*, *z* − 1; (iii) *x* − 1, *y*, *z*.]

Table 3
In vitro activities (MIC_{90} in μ*M*) of **1**-**3**, BTZ043 and its oxidation products.

Data for BTZ043, 'BTZ-SO' and 'BTZ-SO_2' were taken from Tiwari *et al.* (2015).

	1	**2**	**3**	BTZ043	'BTZ-SO'	'BTZ-SO_2' (**4**)
M. tuberculosis	4.3[a]	<0.26[a]	8.0[a]	0.02[b]	0.06[b]	0.48[b]
M. aurum	10.9[c]	2.0[c]	19.4[c]	>200[a]	3.13–12.5[d]	>200[d]

Notes: (*a*) *M. tuberculosis* H_{37}Rv pTEC27 (7H9 medium plus 10% OADC and 0.05% polysorbate 80, microplate RFP assay); (*b*) *M. tuberculosis* H_{37}Rv (7H9 medium plus casitone, palmitic acid, albumin and catalase; MABA, Microplate Alamar Blue Assay); (*c*) *M. aurum* DSMZ 43999 (7H9 medium plus 10% OADC and 0.5% glycerol, microplate OD600 Assay); (*d*) *M. aurum* SB66.

postulated by Szabó *et al.* (1988). We follow these authors in assuming that the anticipated oxidation of **1** to the corresponding BTZ sulfoxide occurred initially and was followed by nucleophilic addition of water (from wet 3-chloroperbenzoic acid used) to the C=N bond of the BTZ system. Ring opening and rearrangement to a sulfenic acid group and an *N*-acylcarbamide moiety within the molecule would be followed by the loss of water to form **2**, which was then oxidized by another equivalent of 3-chloroperbenzoic acid leading to **3**, which we isolated and structurally characterized by X-ray crystallography. Although this mechanism is only postulated, it explains why both **2** and **3** were formed.

3.4. Antimycobacterial activities

Tiwari *et al.* (2015) reported *in vitro* activities of the oxidation products against *Mycobacterium tuberculosis* and *M. aurum*, among other mycobacteria, albeit assuming the BTZ sulfoxide and sulfone structures, which are revised in the present work. We also evaluated the activities of **2** and **3** against *M. tuberculosis* and *M. aurum* (the assay protocols can be found in the supporting information). Although the structures of **2** and **3** differ from those of 'BTZ-SO' and **4** by the absence of the spiro-(2*S*)-methyl-1,3-dioxolane group appended to the piperidine ring in the 4-position, their activities against *M. tuberculosis* and *M. aurum* are comparable (Table 3). Indeed, BITs are known to have antimicrobial activity and are used as preservatives (Novick *et al.*, 2013). Interestingly, BIT **2** and its 1-oxide **3**, as well as 'BTZ-SO' and **4**, show comparable or better activity against both mycobacterial species than the corresponding BTZs **1** and BTZ043 (Table 3). Thus, BITs could likewise be considered as decaprenylphosphoryl-β-D-ribose 2′-epimerase (DprE1) inhibitors, and work along this line is in progess. It should be noted, however, that BITs are known to have various molecular targets in microorganisms (Gopinath *et al.*, 2017). This may render them less promising for the development of antimycobacterial agents.

Acknowledgements

We thank Dr Matthias Schmidt for performing the preparative HPLC of **2** and **3** and Nils Nöthling for the X-ray intensity data collection for **3**. Professor Christian W. Lehmann is gratefully acknowledged for providing access to the X-ray diffraction facility used to collect the data for **3**. AR and HAS would like to thank Professor Yossef Av-Gay for his support. Open access funding enabled and organized by Projekt DEAL.

References

Allen, F. H., Johnson, O., Shields, G. P., Smith, B. R. & Towler, M. (2004). *J. Appl. Cryst.* **37**, 335–338.
Baker, R. J., Colavita, P. E., Murphy, D. M., Platts, J. A. & Wallis, J. D. (2012). *J. Phys. Chem. A*, **116**, 1435–1444.
Bhakuni, B. S., Balkrishna, S. J., Kumar, A. & Kumar, S. (2012). *Tetrahedron Lett.* **53**, 1354–1357.
Brandenburg, K. (2018). *DIAMOND*. Version 3.2k. Crystal Impact GbR, Bonn, Germany.
Bruker (2012). *SADABS*. Bruker AXS Inc., Madison, Wisconsin, USA.
Bruker (2015). *APEX3* and *SAINT*. Bruker AXS Inc., Madison, Wisconsin, USA.

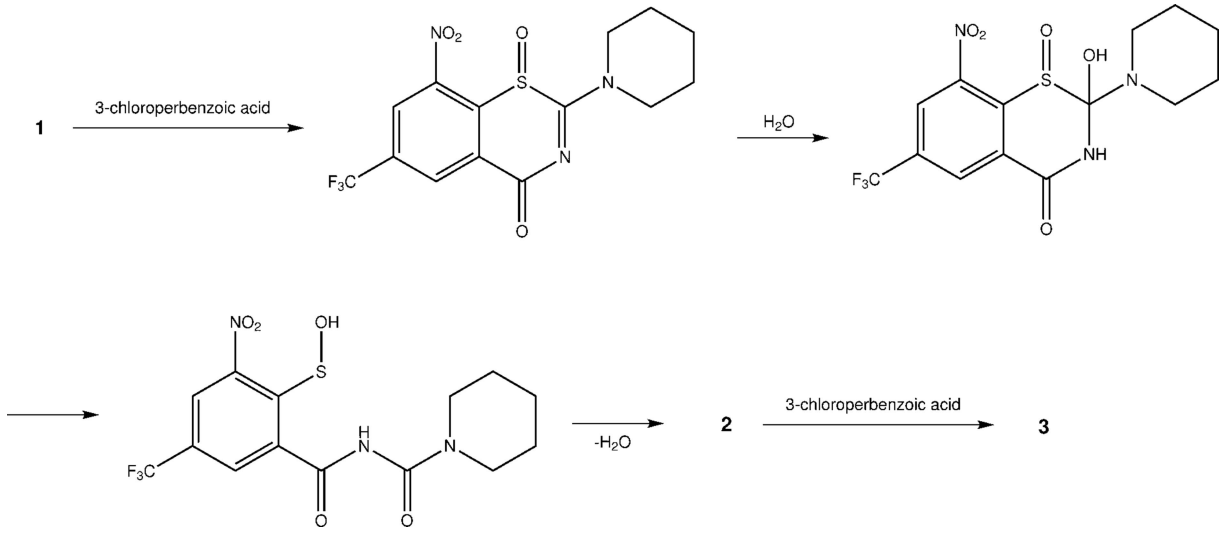

Figure 6
Postulated reaction mechanism for the formation of BITs and BIT 1-oxides from BTZs upon treatment with 3-chloroperbenzoic acid (shown for **1**).

Gopinath, P., Yadav, R. K., Shukla, P. K., Srivastava, K., Puri, S. K. & Muraleedharan, K. M. (2017). *Bioorg. Med. Chem. Lett.* **27**, 1291–1295.
Kloss, F., Krchnak, V., Krchnakova, A., Schieferdecker, S., Dreisbach, J., Krone, V., Möllmann, U., Hoelscher, M. & Miller, M. J. (2017). *Angew. Chem. Int. Ed.* **56**, 2187–2191.
Lupien, A., Vocat, A., Foo, C. S.-Y., Blattes, E., Gillon, J.-Y., Makarov, V. & Cole, S. T. (2018). *Antimicrob. Agents Chemother.* **62**, e00840-18.
Lv, K., You, X., Wang, B., Wei, Z., Chai, Y., Wang, B., Wang, A., Huang, G., Liu, M. & Lu, Y. (2017). *ACS Med. Chem. Lett.* **8**, 636–641.
Makarov, V. & Mikušová, K. (2020). *Appl. Sci.* **10**, 2269.
Mikušová, K., Makarov, V. & Neres, J. (2014). *Curr. Pharm. Des.* **20**, 4379–4403.
Novick, R. M., Nelson, M. L., Unice, K. M., Keenan, J. J. & Paustenbach, D. J. (2013). *Food Chem. Toxicol.* **56**, 60–66.
Parsons, S., Flack, H. D. & Wagner, T. (2013). *Acta Cryst.* B**69**, 249–259.
Rudolph, I., Imming, P. & Richter, A. (2016). Ger. Offen. DE 102014012546 A1 20160331.
Sheldrick, G. M. (2015*a*). *Acta Cryst.* A**71**, 3–8.
Sheldrick, G. M. (2015*b*). *Acta Cryst.* C**71**, 3–8.
Steed, K. M. & Steed, J. W. (2015). *Chem. Rev.* **115**, 2895–2933.
Szabó, J., Szücs, E., Fodor, L., Katócs, Á., Bernáth, G. & Sohár, P. (1988). *Tetrahedron*, **44**, 2985–2992.
Tiwari, R., Miller, P. A., Cho, S., Franzblau, S. G. & Miller, M. J. (2015). *ACS Med. Chem. Lett.* **6**, 128–133.
Tiwari, R., Moraski, G. C., Krchňák, V., Miller, P. A., Colon-Martinez, M., Herrero, E., Oliver, A. G. & Miller, M. J. (2013). *J. Am. Chem. Soc.* **135**, 3539–3549.
Westrip, S. P. (2010). *J. Appl. Cryst.* **43**, 920–925.
Zhang, G. & Aldrich, C. C. (2019). *Acta Cryst.* C**75**, 1031–1035.
Zhang, G., Howe, M. & Aldrich, C. A. (2019). *ACS Med. Chem. Lett.* **10**, 348–351.

supporting information

Acta Cryst. (2020). C**76**, 907-913 [https://doi.org/10.1107/S2053229620010931]

Crystallographic evidence for unintended benzisothiazolinone 1-oxide formation from benzothiazinones through oxidation

Tamira Eckhardt, Richard Goddard, Christoph Lehmann, Adrian Richter, Henok Asfaw Sahile, Rui Liu, Rohit Tiwari, Allen G. Oliver, Marvin J. Miller, Rüdiger W. Seidel and Peter Imming

Computing details

For both structures, data collection: *APEX3* (Bruker, 2015); cell refinement: *SAINT* (Bruker, 2015); data reduction: *SAINT* (Bruker, 2015); program(s) used to solve structure: SHELXT (Sheldrick, 2015a); program(s) used to refine structure: *SHELXL2018* (Sheldrick, 2015b); molecular graphics: *DIAMOND* (Brandenburg, 2018); software used to prepare material for publication: *enCIFer* (Allen *et al.*, 2004) and *publCIF* (Westrip, 2010).

7-Nitro-2-(piperidine-1-carbonyl)-5-(trifluoromethyl)benzo[*d*]isothiazol-3(2*H*)-one 1-oxide (3)

Crystal data

$C_{14}H_{12}F_3N_3O_5S$
M_r = 391.33
Orthorhombic, *Iba*2
a = 17.6719 (8) Å
b = 25.7296 (12) Å
c = 6.8887 (3) Å
V = 3132.2 (2) Å^3
Z = 8
F(000) = 1600
D_x = 1.660 Mg m^{-3}
Cu *Kα* radiation, *λ* = 1.54178 Å
Cell parameters from 2591 reflections
θ = 3.0–47.9°
μ = 2.50 mm^{-1}
T = 100 K
Needle, yellow
0.23 × 0.06 × 0.04 mm

Data collection

Bruker Kappa Mach3 APEXII diffractometer
Radiation source: 0.2 x 2mm^2 focus rotating anode
MONTEL graded multilayer optics monochromator
Detector resolution: 66.67 pixels mm^{-1}
φ– and *ω*–scans
Absorption correction: gaussian (SADABS; Bruker, 2012)
T_{min} = 0.748, T_{max} = 0.936
22457 measured reflections
2477 independent reflections
1843 reflections with $I > 2\sigma(I)$
R_{int} = 0.102
θ_{max} = 70.1°, θ_{min} = 3.0°
h = −20→18
k = −29→29
l = −7→7

Refinement

Refinement on F^2
Least-squares matrix: full
$R[F^2 > 2\sigma(F^2)]$ = 0.059
$wR(F^2)$ = 0.170
S = 1.08
2477 reflections
235 parameters
1 restraint
Primary atom site location: dual
Secondary atom site location: difference Fourier map
Hydrogen site location: inferred from neighbouring sites
H-atom parameters constrained

$w = 1/[\sigma^2(F_o^2) + (0.0581P)^2 + 17.2243P]$
where $P = (F_o^2 + 2F_c^2)/3$
$(\Delta/\sigma)_{max} < 0.001$
$\Delta\rho_{max} = 0.53$ e Å^{-3}
$\Delta\rho_{min} = -0.75$ e Å^{-3}

Absolute structure: Flack *x* determined using 550 quotients [(I+)-(I-)]/[(I+)+(I-)] (Parsons *et al.*, 2013)
Absolute structure parameter: 0.08 (5)

Special details

Geometry. All esds (except the esd in the dihedral angle between two l.s. planes) are estimated using the full covariance matrix. The cell esds are taken into account individually in the estimation of esds in distances, angles and torsion angles; correlations between esds in cell parameters are only used when they are defined by crystal symmetry. An approximate (isotropic) treatment of cell esds is used for estimating esds involving l.s. planes.

Fractional atomic coordinates and isotropic or equivalent isotropic displacement parameters (Å²)

	x	*y*	*z*	U_{iso}*/U_{eq}
S1	0.39270 (11)	0.23902 (8)	0.2946 (4)	0.0263 (5)
F1	0.2738 (3)	0.4716 (2)	0.6178 (10)	0.0484 (17)
F2	0.3923 (3)	0.4791 (2)	0.6776 (10)	0.0498 (17)
F3	0.3204 (4)	0.4389 (2)	0.8789 (9)	0.0471 (17)
O1	0.4744 (3)	0.2295 (2)	0.2901 (11)	0.0306 (14)
O2	0.2793 (3)	0.2404 (2)	0.7694 (9)	0.0298 (15)
O3	0.4304 (4)	0.3133 (3)	0.0182 (11)	0.0428 (18)
O4	0.4590 (4)	0.3947 (3)	0.0606 (12)	0.0478 (19)
O5	0.3327 (3)	0.1386 (2)	0.3621 (9)	0.0308 (16)
N2	0.3585 (4)	0.2155 (3)	0.5159 (11)	0.0242 (17)
N3	0.4310 (4)	0.3531 (3)	0.1142 (12)	0.035 (2)
N4	0.3505 (4)	0.1367 (3)	0.6918 (11)	0.0244 (16)
C3	0.3214 (5)	0.2512 (3)	0.6345 (14)	0.027 (2)
C3A	0.3407 (4)	0.3036 (4)	0.5686 (14)	0.027 (2)
C4	0.3244 (5)	0.3493 (3)	0.6639 (14)	0.027 (2)
H4	0.297101	0.348687	0.782699	0.033*
C5	0.3480 (5)	0.3961 (4)	0.5857 (15)	0.029 (2)
C6	0.3843 (5)	0.3979 (4)	0.4055 (15)	0.030 (2)
H6	0.399673	0.430018	0.350254	0.036*
C7	0.3970 (5)	0.3513 (3)	0.3099 (16)	0.0262 (19)
C7A	0.3775 (5)	0.3036 (4)	0.3912 (14)	0.028 (2)
C8	0.3337 (6)	0.4459 (4)	0.6897 (18)	0.038 (3)
C9	0.3460 (5)	0.1602 (3)	0.5197 (15)	0.029 (2)
C10	0.3233 (5)	0.0826 (4)	0.7055 (15)	0.032 (2)
H10A	0.309365	0.070047	0.574432	0.039*
H10B	0.277370	0.081524	0.787702	0.039*
C11	0.3836 (5)	0.0469 (3)	0.7919 (18)	0.034 (2)
H11A	0.361581	0.011974	0.813779	0.041*
H11B	0.425884	0.043181	0.698612	0.041*
C12	0.4138 (6)	0.0681 (4)	0.9830 (15)	0.033 (2)
H12A	0.455499	0.045824	1.030461	0.040*
H12B	0.373036	0.068011	1.081686	0.040*
C13	0.4426 (5)	0.1238 (3)	0.9521 (14)	0.028 (2)
H13A	0.460546	0.137967	1.077522	0.033*

H13B	0.486071	0.123146	0.861508	0.033*
C14	0.3822 (5)	0.1587 (4)	0.8718 (15)	0.032 (2)
H14A	0.341411	0.162932	0.968949	0.039*
H14B	0.403903	0.193404	0.844520	0.039*

Atomic displacement parameters (Å²)

	U^{11}	U^{22}	U^{33}	U^{12}	U^{13}	U^{23}
S1	0.0261 (10)	0.0301 (10)	0.0225 (11)	0.0024 (8)	0.0004 (10)	−0.0012 (11)
F1	0.045 (3)	0.035 (3)	0.065 (5)	0.014 (3)	−0.003 (3)	−0.012 (3)
F2	0.047 (4)	0.035 (3)	0.067 (5)	−0.011 (3)	0.004 (3)	−0.011 (3)
F3	0.062 (4)	0.038 (3)	0.040 (4)	−0.001 (3)	0.009 (3)	−0.009 (3)
O1	0.026 (3)	0.036 (3)	0.030 (4)	0.006 (2)	0.001 (3)	0.004 (3)
O2	0.031 (3)	0.032 (3)	0.027 (4)	0.002 (3)	0.008 (3)	0.001 (3)
O3	0.055 (5)	0.045 (5)	0.029 (4)	0.013 (4)	0.005 (4)	0.001 (3)
O4	0.047 (4)	0.049 (4)	0.048 (5)	0.003 (4)	0.021 (4)	0.010 (4)
O5	0.033 (4)	0.032 (4)	0.027 (4)	0.001 (3)	−0.006 (3)	−0.004 (3)
N2	0.021 (4)	0.029 (4)	0.022 (4)	0.002 (3)	−0.001 (3)	−0.004 (3)
N3	0.035 (5)	0.036 (5)	0.034 (5)	0.006 (4)	0.012 (4)	0.011 (4)
N4	0.033 (4)	0.022 (4)	0.019 (4)	−0.002 (3)	−0.007 (3)	0.002 (3)
C3	0.020 (5)	0.038 (5)	0.024 (6)	0.005 (4)	0.000 (4)	−0.004 (4)
C3A	0.016 (4)	0.034 (5)	0.030 (6)	0.003 (4)	−0.007 (4)	−0.002 (4)
C4	0.023 (5)	0.033 (5)	0.026 (6)	0.007 (4)	0.006 (4)	−0.011 (4)
C5	0.022 (4)	0.030 (5)	0.033 (6)	0.001 (4)	−0.002 (4)	−0.001 (4)
C6	0.020 (4)	0.029 (5)	0.040 (6)	0.004 (4)	0.004 (4)	0.004 (4)
C7	0.025 (4)	0.028 (4)	0.025 (5)	0.002 (4)	0.006 (4)	0.005 (5)
C7A	0.016 (4)	0.041 (6)	0.026 (5)	0.000 (4)	0.005 (4)	0.000 (4)
C8	0.031 (5)	0.039 (6)	0.045 (8)	−0.004 (5)	0.007 (5)	0.003 (5)
C9	0.027 (5)	0.029 (5)	0.030 (6)	0.002 (4)	−0.001 (4)	−0.001 (5)
C10	0.023 (5)	0.040 (5)	0.034 (6)	−0.004 (4)	−0.004 (4)	−0.006 (4)
C11	0.038 (5)	0.025 (5)	0.041 (6)	0.002 (4)	−0.001 (5)	0.005 (5)
C12	0.037 (6)	0.028 (5)	0.034 (6)	−0.001 (4)	−0.007 (4)	0.008 (4)
C13	0.032 (5)	0.026 (5)	0.026 (6)	0.002 (4)	0.001 (4)	−0.003 (4)
C14	0.031 (5)	0.031 (5)	0.034 (6)	−0.002 (4)	−0.004 (5)	0.003 (4)

Geometric parameters (Å, º)

S1—O1	1.465 (6)	C4—H4	0.9500
S1—N2	1.748 (8)	C5—C6	1.398 (14)
S1—C7A	1.810 (10)	C5—C8	1.490 (14)
F1—C8	1.344 (12)	C6—C7	1.386 (13)
F2—C8	1.345 (11)	C6—H6	0.9500
F3—C8	1.336 (13)	C7—C7A	1.393 (12)
O2—C3	1.222 (11)	C10—C11	1.529 (13)
O3—N3	1.220 (11)	C10—H10A	0.9900
O4—N3	1.236 (10)	C10—H10B	0.9900
O5—C9	1.243 (12)	C11—C12	1.522 (15)
N2—C3	1.394 (11)	C11—H11A	0.9900

N2—C9	1.439 (11)	C11—H11B	0.9900
N3—C7	1.477 (13)	C12—C13	1.535 (12)
N4—C9	1.334 (12)	C12—H12A	0.9900
N4—C14	1.474 (12)	C12—H12B	0.9900
N4—C10	1.474 (11)	C13—C14	1.500 (12)
C3—C3A	1.461 (13)	C13—H13A	0.9900
C3A—C4	1.378 (12)	C13—H13B	0.9900
C3A—C7A	1.384 (14)	C14—H14A	0.9900
C4—C5	1.384 (12)	C14—H14B	0.9900

O1—S1—N2	107.6 (4)	F3—C8—C5	112.5 (9)
O1—S1—C7A	107.9 (4)	F1—C8—C5	112.4 (9)
N2—S1—C7A	86.9 (4)	F2—C8—C5	112.7 (8)
C3—N2—C9	124.7 (8)	O5—C9—N4	125.7 (8)
C3—N2—S1	116.4 (6)	O5—C9—N2	117.1 (9)
C9—N2—S1	114.3 (6)	N4—C9—N2	117.1 (8)
O3—N3—O4	124.7 (9)	N4—C10—C11	111.4 (7)
O3—N3—C7	117.7 (8)	N4—C10—H10A	109.3
O4—N3—C7	117.6 (8)	C11—C10—H10A	109.3
C9—N4—C14	126.6 (7)	N4—C10—H10B	109.3
C9—N4—C10	117.8 (8)	C11—C10—H10B	109.3
C14—N4—C10	115.6 (7)	H10A—C10—H10B	108.0
O2—C3—N2	125.5 (9)	C12—C11—C10	111.4 (8)
O2—C3—C3A	126.0 (8)	C12—C11—H11A	109.4
N2—C3—C3A	108.4 (8)	C10—C11—H11A	109.4
C4—C3A—C7A	121.2 (9)	C12—C11—H11B	109.4
C4—C3A—C3	126.1 (9)	C10—C11—H11B	109.4
C7A—C3A—C3	112.7 (8)	H11A—C11—H11B	108.0
C3A—C4—C5	119.7 (9)	C11—C12—C13	109.4 (8)
C3A—C4—H4	120.2	C11—C12—H12A	109.8
C5—C4—H4	120.2	C13—C12—H12A	109.8
C4—C5—C6	120.8 (9)	C11—C12—H12B	109.8
C4—C5—C8	120.7 (9)	C13—C12—H12B	109.8
C6—C5—C8	118.5 (9)	H12A—C12—H12B	108.2
C7—C6—C5	117.9 (9)	C14—C13—C12	111.9 (8)
C7—C6—H6	121.0	C14—C13—H13A	109.2
C5—C6—H6	121.0	C12—C13—H13A	109.2
C6—C7—C7A	122.1 (9)	C14—C13—H13B	109.2
C6—C7—N3	118.2 (8)	C12—C13—H13B	109.2
C7A—C7—N3	119.7 (8)	H13A—C13—H13B	107.9
C3A—C7A—C7	118.2 (9)	N4—C14—C13	110.5 (8)
C3A—C7A—S1	113.2 (7)	N4—C14—H14A	109.5
C7—C7A—S1	128.6 (7)	C13—C14—H14A	109.5
F3—C8—F1	106.7 (8)	N4—C14—H14B	109.5
F3—C8—F2	106.3 (9)	C13—C14—H14B	109.5
F1—C8—F2	105.8 (8)	H14A—C14—H14B	108.1

O1—S1—N2—C3	121.9 (6)	N3—C7—C7A—C3A	−175.3 (8)

C7A—S1—N2—C3	14.1 (6)	C6—C7—C7A—S1	−177.4 (7)
O1—S1—N2—C9	−80.9 (6)	N3—C7—C7A—S1	3.8 (13)
C7A—S1—N2—C9	171.3 (6)	O1—S1—C7A—C3A	−114.4 (7)
C9—N2—C3—O2	7.5 (14)	N2—S1—C7A—C3A	−6.9 (7)
S1—N2—C3—O2	162.1 (7)	O1—S1—C7A—C7	66.4 (9)
C9—N2—C3—C3A	−171.7 (8)	N2—S1—C7A—C7	173.9 (9)
S1—N2—C3—C3A	−17.1 (9)	C4—C5—C8—F3	20.3 (13)
O2—C3—C3A—C4	10.7 (14)	C6—C5—C8—F3	−161.2 (8)
N2—C3—C3A—C4	−170.1 (8)	C4—C5—C8—F1	−100.2 (11)
O2—C3—C3A—C7A	−168.2 (9)	C6—C5—C8—F1	78.4 (11)
N2—C3—C3A—C7A	11.0 (10)	C4—C5—C8—F2	140.5 (9)
C7A—C3A—C4—C5	−2.8 (13)	C6—C5—C8—F2	−41.0 (13)
C3—C3A—C4—C5	178.3 (8)	C14—N4—C9—O5	165.6 (8)
C3A—C4—C5—C6	3.8 (13)	C10—N4—C9—O5	−12.6 (13)
C3A—C4—C5—C8	−177.7 (9)	C14—N4—C9—N2	−13.8 (13)
C4—C5—C6—C7	−1.2 (13)	C10—N4—C9—N2	168.1 (7)
C8—C5—C6—C7	−179.7 (8)	C3—N2—C9—O5	128.9 (9)
C5—C6—C7—C7A	−2.5 (13)	S1—N2—C9—O5	−26.2 (10)
C5—C6—C7—N3	176.4 (8)	C3—N2—C9—N4	−51.7 (12)
O3—N3—C7—C6	−167.9 (8)	S1—N2—C9—N4	153.3 (7)
O4—N3—C7—C6	13.0 (12)	C9—N4—C10—C11	126.6 (9)
O3—N3—C7—C7A	10.9 (13)	C14—N4—C10—C11	−51.8 (11)
O4—N3—C7—C7A	−168.1 (8)	N4—C10—C11—C12	52.2 (11)
C4—C3A—C7A—C7	−0.8 (13)	C10—C11—C12—C13	−54.9 (11)
C3—C3A—C7A—C7	178.2 (8)	C11—C12—C13—C14	57.0 (11)
C4—C3A—C7A—S1	180.0 (7)	C9—N4—C14—C13	−125.1 (10)
C3—C3A—C7A—S1	−1.1 (10)	C10—N4—C14—C13	53.0 (10)
C6—C7—C7A—C3A	3.5 (13)	C12—C13—C14—N4	−54.9 (10)

2-[(*S*)-2-Methyl-1,4-dioxa-8-azaspiro[4.5]decane-8-carbonyl]-7-nitro-5-(trifluoromethyl)benzo[*d*]isothiazol-3(2*H*)-one 1-oxide (4)

Crystal data

$C_{17}H_{16}F_3N_3O_7S$
M_r = 463.39
Monoclinic, $P2_1$
a = 8.8165 (2) Å
b = 16.1649 (4) Å
c = 13.4246 (3) Å
β = 90.0022 (12)°
V = 1913.24 (8) Å^3
Z = 4
$F(000)$ = 952
D_x = 1.609 Mg m^{-3}
Cu $K\alpha$ radiation, λ = 1.54178 Å
Cell parameters from 9779 reflections
θ = 3.3–70.3°
μ = 2.23 mm^{-1}
T = 120 K
Blade, colorless
0.25 × 0.07 × 0.04 mm

Data collection

Bruker PHOTON-II diffractometer
Radiation source: Incoatec micro-focus
Detector resolution: 7.41 pixels mm^{-1}
φ– and ω–scans
Absorption correction: numerical (SADABS; Bruker, 2012)
T_{min} = 0.715, T_{max} = 0.949
36857 measured reflections
7140 independent reflections
6860 reflections with $I > 2\sigma(I)$

R_{int} = 0.041
θ_{max} = 70.3°, θ_{min} = 3.3°
h = −10→10
k = −19→19
l = −16→16

Refinement

Refinement on F^2
Least-squares matrix: full
$R[F^2 > 2\sigma(F^2)]$ = 0.033
$wR(F^2)$ = 0.083
S = 1.04
7140 reflections
561 parameters
1 restraint
Primary atom site location: dual
Secondary atom site location: difference Fourier map
Hydrogen site location: inferred from neighbouring sites
H-atom parameters constrained
$w = 1/[\sigma^2(F_o^2) + (0.0446P)^2 + 0.5798P]$ where $P = (F_o^2 + 2F_c^2)/3$
$(\Delta/\sigma)_{max} < 0.001$
$\Delta\rho_{max}$ = 0.61 e Å^{-3}
$\Delta\rho_{min}$ = −0.31 e Å^{-3}
Absolute structure: Flack x determined using 3080 quotients [(I+)-(I-)]/[(I+)+(I-)] (Parsons *et al.*, 2013)
Absolute structure parameter: 0.017 (6)

Special details

Geometry. All esds (except the esd in the dihedral angle between two l.s. planes) are estimated using the full covariance matrix. The cell esds are taken into account individually in the estimation of esds in distances, angles and torsion angles; correlations between esds in cell parameters are only used when they are defined by crystal symmetry. An approximate (isotropic) treatment of cell esds is used for estimating esds involving l.s. planes.

Refinement. Although the monoclinic beta angle is close to 90°, the structure is monoclinic with no sign of twinning. Averaging the diffraction data under mmm Laue symmetry results in R(sym) = 0.305 (XPREP).

Fractional atomic coordinates and isotropic or equivalent isotropic displacement parameters (Å²)

	x	y	z	U_{iso}*/U_{eq}
S1_1	0.30602 (8)	0.66421 (5)	0.53028 (5)	0.02508 (16)
F1_1	0.4878 (3)	0.5408 (2)	0.0698 (2)	0.0671 (9)
F2_1	0.3554 (4)	0.43821 (16)	0.11563 (19)	0.0611 (8)
F3_1	0.2495 (4)	0.5428 (2)	0.05546 (19)	0.0698 (9)
O1_1	0.1439 (2)	0.66606 (16)	0.55526 (16)	0.0311 (5)
O2_1	0.4782 (3)	0.44663 (16)	0.50398 (18)	0.0351 (6)
O3_1	0.2457 (4)	0.79269 (17)	0.4081 (2)	0.0440 (6)
O4_1	0.1989 (3)	0.79614 (17)	0.2497 (2)	0.0411 (6)
O5_1	0.4618 (3)	0.62275 (15)	0.70901 (17)	0.0303 (5)
O6_1	0.2306 (3)	0.33735 (16)	0.8664 (2)	0.0355 (6)
O7_1	0.4331 (3)	0.25355 (16)	0.8326 (2)	0.0372 (6)
N2_1	0.3682 (3)	0.56598 (17)	0.5661 (2)	0.0257 (6)
N3_1	0.2405 (3)	0.76066 (18)	0.3254 (2)	0.0321 (6)
N4_1	0.3743 (3)	0.49099 (18)	0.7162 (2)	0.0272 (6)
C3_1	0.4135 (4)	0.5114 (2)	0.4911 (2)	0.0270 (7)
C3A_1	0.3715 (4)	0.5490 (2)	0.3938 (2)	0.0251 (6)
C4_1	0.3832 (3)	0.5100 (2)	0.3017 (2)	0.0251 (6)
H4_1	0.413697	0.453809	0.296739	0.030*
C5_1	0.3484 (3)	0.5563 (2)	0.2168 (2)	0.0256 (6)
C6_1	0.3028 (4)	0.6385 (2)	0.2245 (2)	0.0278 (7)
H6_1	0.280891	0.669736	0.166306	0.033*
C7_1	0.2897 (3)	0.6742 (2)	0.3177 (2)	0.0261 (6)

C7A_1	0.3224 (3)	0.6294 (2)	0.4026 (2)	0.0243 (6)
C8_1	0.3641 (4)	0.5181 (2)	0.1151 (2)	0.0300 (7)
C9_1	0.4068 (4)	0.5614 (2)	0.6702 (2)	0.0262 (6)
C10_1	0.4126 (4)	0.4841 (2)	0.8225 (2)	0.0300 (7)
H10A_1	0.320432	0.493256	0.863078	0.036*
H10B_1	0.487716	0.527145	0.840268	0.036*
C11_1	0.4776 (4)	0.3993 (2)	0.8452 (3)	0.0319 (7)
H11A_1	0.576074	0.392673	0.810696	0.038*
H11B_1	0.495561	0.394122	0.917723	0.038*
C12_1	0.3696 (4)	0.3320 (2)	0.8115 (3)	0.0305 (7)
C13_1	0.3324 (4)	0.3413 (2)	0.7007 (3)	0.0318 (7)
H13A_1	0.425391	0.333099	0.660625	0.038*
H13B_1	0.257375	0.298890	0.680770	0.038*
C14_1	0.2686 (4)	0.4268 (2)	0.6816 (3)	0.0305 (7)
H14A_1	0.249873	0.433853	0.609366	0.037*
H14B_1	0.170498	0.432827	0.716744	0.037*
C15_1	0.2153 (4)	0.2645 (2)	0.9264 (3)	0.0357 (8)
H15_1	0.258964	0.274399	0.994133	0.043*
C16_1	0.3134 (4)	0.2035 (2)	0.8696 (3)	0.0387 (8)
H16A_1	0.352563	0.159634	0.914125	0.046*
H16B_1	0.255997	0.177567	0.814418	0.046*
C17_1	0.0503 (5)	0.2413 (3)	0.9349 (3)	0.0409 (9)
H17A_1	−0.003992	0.284440	0.971850	0.061*
H17B_1	0.041028	0.188541	0.970358	0.061*
H17C_1	0.006466	0.235913	0.868172	0.061*
S1_2	0.80116 (8)	0.67422 (5)	0.49508 (5)	0.02466 (16)
F1_2	0.9905 (3)	0.52933 (17)	0.94230 (18)	0.0502 (6)
F2_2	0.8580 (3)	0.42752 (15)	0.89242 (16)	0.0505 (6)
F3_2	0.7516 (3)	0.5301 (2)	0.96310 (18)	0.0598 (8)
O1_2	0.6391 (3)	0.67522 (16)	0.46951 (17)	0.0314 (5)
O2_2	0.9930 (3)	0.46106 (16)	0.50856 (17)	0.0317 (5)
O3_2	0.7350 (3)	0.79653 (17)	0.6287 (2)	0.0416 (6)
O4_2	0.6666 (3)	0.78627 (17)	0.7835 (2)	0.0387 (6)
O5_2	0.9631 (3)	0.63962 (15)	0.31252 (17)	0.0312 (5)
O6_2	0.7628 (3)	0.34331 (14)	0.15282 (17)	0.0278 (5)
O7_2	0.9657 (3)	0.26758 (15)	0.19997 (19)	0.0310 (5)
N2_2	0.8690 (3)	0.57884 (17)	0.4538 (2)	0.0250 (5)
N3_2	0.7211 (3)	0.75800 (18)	0.7071 (2)	0.0299 (6)
N4_2	0.8767 (3)	0.50701 (17)	0.30231 (19)	0.0258 (5)
C3_2	0.9198 (4)	0.5226 (2)	0.5250 (2)	0.0253 (6)
C3A_2	0.8723 (3)	0.5537 (2)	0.6242 (2)	0.0237 (6)
C4_2	0.8831 (3)	0.5105 (2)	0.7132 (2)	0.0244 (6)
H4_2	0.917693	0.454873	0.714581	0.029*
C5_2	0.8417 (4)	0.5513 (2)	0.8004 (2)	0.0253 (6)
C6_2	0.7886 (3)	0.6322 (2)	0.7985 (2)	0.0256 (6)
H6_2	0.760764	0.659404	0.858474	0.031*
C7_2	0.7769 (3)	0.6725 (2)	0.7080 (2)	0.0256 (6)
C7A_2	0.8166 (3)	0.6337 (2)	0.6208 (2)	0.0243 (6)

C8_2	0.8602 (4)	0.5086 (2)	0.8995 (2)	0.0278 (7)
C9_2	0.9082 (3)	0.5775 (2)	0.3495 (2)	0.0247 (6)
C10_2	0.9211 (4)	0.4984 (2)	0.1973 (2)	0.0286 (7)
H10C_2	0.992716	0.543109	0.179110	0.034*
H10D_2	0.830364	0.503397	0.154230	0.034*
C11_2	0.9963 (4)	0.4141 (2)	0.1808 (2)	0.0296 (7)
H11C_2	1.019612	0.407034	0.109177	0.036*
H11D_2	1.092943	0.411788	0.218231	0.036*
C12_2	0.8936 (4)	0.3445 (2)	0.2150 (2)	0.0267 (7)
C13_2	0.8496 (4)	0.3570 (2)	0.3241 (2)	0.0279 (7)
H13C_2	0.778394	0.312906	0.344953	0.033*
H13D_2	0.941200	0.353360	0.366559	0.033*
C14_2	0.7756 (4)	0.4407 (2)	0.3373 (2)	0.0277 (7)
H14C_2	0.679456	0.442399	0.299286	0.033*
H14D_2	0.751547	0.449476	0.408546	0.033*
C15_2	0.7050 (4)	0.2603 (2)	0.1594 (3)	0.0294 (7)
H15B_2	0.632899	0.255825	0.216599	0.035*
C16_2	0.8482 (4)	0.2086 (2)	0.1806 (3)	0.0307 (7)
H16C_2	0.832426	0.172305	0.239069	0.037*
H16D_2	0.874416	0.173854	0.122391	0.037*
C17_2	0.6243 (5)	0.2395 (3)	0.0633 (3)	0.0399 (9)
H17D_2	0.535456	0.275423	0.055739	0.060*
H17E_2	0.591606	0.181582	0.064828	0.060*
H17F_2	0.693369	0.248058	0.007064	0.060*

Atomic displacement parameters (Å²)

	U^{11}	U^{22}	U^{33}	U^{12}	U^{13}	U^{23}
S1_1	0.0265 (4)	0.0257 (4)	0.0231 (3)	−0.0001 (3)	0.0001 (2)	−0.0018 (3)
F1_1	0.0607 (17)	0.085 (2)	0.0554 (16)	−0.0381 (15)	0.0340 (13)	−0.0312 (15)
F2_1	0.108 (2)	0.0411 (14)	0.0342 (12)	−0.0178 (14)	0.0175 (13)	−0.0051 (10)
F3_1	0.0717 (19)	0.104 (2)	0.0339 (13)	0.0250 (17)	−0.0134 (12)	−0.0137 (14)
O1_1	0.0277 (11)	0.0361 (12)	0.0295 (11)	0.0008 (10)	0.0046 (8)	−0.0032 (11)
O2_1	0.0442 (15)	0.0354 (14)	0.0256 (12)	0.0118 (11)	0.0011 (10)	0.0025 (10)
O3_1	0.0616 (18)	0.0320 (13)	0.0383 (15)	0.0057 (12)	−0.0041 (12)	−0.0014 (11)
O4_1	0.0498 (16)	0.0341 (13)	0.0394 (15)	0.0042 (12)	−0.0013 (12)	0.0121 (12)
O5_1	0.0313 (12)	0.0327 (13)	0.0269 (12)	−0.0043 (10)	−0.0019 (9)	−0.0024 (10)
O6_1	0.0355 (13)	0.0308 (12)	0.0403 (14)	0.0049 (10)	0.0104 (10)	0.0064 (10)
O7_1	0.0356 (14)	0.0310 (13)	0.0450 (15)	0.0076 (10)	−0.0017 (11)	0.0009 (11)
N2_1	0.0293 (14)	0.0266 (14)	0.0213 (13)	0.0028 (10)	−0.0002 (10)	0.0006 (10)
N3_1	0.0345 (16)	0.0279 (14)	0.0339 (16)	0.0000 (12)	0.0023 (12)	0.0070 (13)
N4_1	0.0302 (14)	0.0314 (15)	0.0201 (13)	−0.0038 (11)	−0.0022 (10)	−0.0010 (11)
C3_1	0.0274 (16)	0.0316 (18)	0.0221 (15)	0.0019 (13)	0.0007 (11)	0.0020 (13)
C3A_1	0.0225 (15)	0.0281 (16)	0.0247 (15)	−0.0007 (12)	0.0001 (11)	0.0044 (13)
C4_1	0.0218 (14)	0.0280 (16)	0.0255 (16)	−0.0001 (12)	0.0028 (11)	−0.0004 (12)
C5_1	0.0209 (15)	0.0323 (16)	0.0235 (15)	−0.0057 (12)	0.0026 (11)	0.0022 (13)
C6_1	0.0232 (15)	0.0346 (17)	0.0255 (16)	−0.0042 (13)	0.0011 (11)	0.0056 (13)
C7_1	0.0231 (14)	0.0262 (15)	0.0290 (15)	−0.0041 (13)	0.0009 (11)	0.0010 (14)

C7A_1	0.0205 (14)	0.0282 (16)	0.0242 (15)	−0.0038 (12)	0.0018 (11)	0.0006 (12)
C8_1	0.0343 (18)	0.0325 (18)	0.0231 (16)	−0.0071 (14)	0.0047 (12)	0.0041 (13)
C9_1	0.0215 (15)	0.0340 (17)	0.0232 (15)	0.0024 (12)	0.0010 (11)	−0.0023 (13)
C10_1	0.0325 (18)	0.0358 (19)	0.0216 (15)	−0.0007 (14)	−0.0034 (12)	−0.0015 (13)
C11_1	0.0322 (18)	0.0375 (19)	0.0259 (16)	0.0016 (14)	−0.0043 (13)	0.0000 (14)
C12_1	0.0294 (17)	0.0330 (17)	0.0292 (17)	0.0024 (14)	0.0025 (13)	−0.0007 (13)
C13_1	0.0313 (17)	0.0339 (18)	0.0302 (17)	−0.0019 (14)	−0.0029 (13)	−0.0062 (14)
C14_1	0.0269 (17)	0.0356 (18)	0.0289 (16)	−0.0039 (14)	−0.0046 (13)	−0.0003 (14)
C15_1	0.040 (2)	0.0369 (19)	0.0306 (18)	−0.0008 (15)	−0.0060 (14)	0.0088 (15)
C16_1	0.038 (2)	0.0299 (17)	0.048 (2)	0.0023 (14)	−0.0051 (16)	0.0084 (16)
C17_1	0.042 (2)	0.040 (2)	0.041 (2)	−0.0031 (16)	0.0030 (16)	0.0087 (16)
S1_2	0.0262 (4)	0.0249 (4)	0.0229 (3)	0.0013 (3)	−0.0001 (2)	0.0016 (3)
F1_2	0.0472 (13)	0.0622 (15)	0.0411 (13)	−0.0194 (11)	−0.0207 (10)	0.0156 (11)
F2_2	0.089 (2)	0.0348 (12)	0.0277 (11)	−0.0093 (12)	−0.0064 (11)	0.0037 (9)
F3_2	0.0599 (16)	0.090 (2)	0.0293 (12)	0.0263 (15)	0.0181 (11)	0.0136 (12)
O1_2	0.0281 (11)	0.0358 (12)	0.0303 (11)	0.0032 (10)	−0.0041 (8)	0.0019 (11)
O2_2	0.0371 (13)	0.0344 (13)	0.0236 (11)	0.0105 (10)	−0.0014 (9)	−0.0023 (9)
O3_2	0.0545 (17)	0.0306 (13)	0.0398 (15)	0.0085 (12)	−0.0005 (12)	0.0009 (12)
O4_2	0.0359 (14)	0.0376 (14)	0.0425 (15)	0.0036 (11)	0.0047 (11)	−0.0128 (11)
O5_2	0.0359 (13)	0.0322 (12)	0.0253 (11)	−0.0054 (10)	0.0045 (9)	0.0018 (9)
O6_2	0.0274 (12)	0.0309 (12)	0.0251 (11)	0.0000 (9)	−0.0029 (9)	0.0013 (9)
O7_2	0.0259 (12)	0.0286 (12)	0.0384 (13)	0.0027 (9)	−0.0011 (9)	−0.0020 (10)
N2_2	0.0286 (13)	0.0263 (14)	0.0202 (13)	0.0015 (11)	0.0008 (10)	−0.0010 (10)
N3_2	0.0282 (15)	0.0272 (14)	0.0343 (16)	0.0006 (11)	−0.0024 (11)	−0.0077 (12)
N4_2	0.0267 (13)	0.0299 (14)	0.0206 (13)	−0.0018 (11)	0.0033 (10)	0.0014 (11)
C3_2	0.0275 (16)	0.0271 (16)	0.0214 (14)	0.0008 (13)	−0.0006 (11)	−0.0017 (12)
C3A_2	0.0215 (15)	0.0283 (16)	0.0213 (15)	0.0002 (12)	−0.0001 (11)	−0.0027 (12)
C4_2	0.0216 (14)	0.0282 (16)	0.0236 (15)	0.0007 (12)	0.0000 (11)	−0.0006 (12)
C5_2	0.0215 (15)	0.0336 (17)	0.0206 (15)	−0.0049 (12)	−0.0001 (11)	−0.0006 (13)
C6_2	0.0214 (14)	0.0310 (16)	0.0244 (15)	−0.0016 (12)	0.0010 (11)	−0.0054 (13)
C7_2	0.0194 (13)	0.0268 (15)	0.0306 (15)	−0.0011 (13)	0.0000 (11)	−0.0050 (14)
C7A_2	0.0209 (14)	0.0269 (15)	0.0251 (15)	−0.0030 (12)	−0.0011 (11)	0.0015 (12)
C8_2	0.0274 (16)	0.0344 (18)	0.0215 (15)	−0.0023 (13)	0.0004 (12)	−0.0017 (13)
C9_2	0.0219 (14)	0.0323 (17)	0.0199 (14)	0.0025 (12)	−0.0001 (11)	0.0027 (12)
C10_2	0.0337 (17)	0.0311 (17)	0.0211 (15)	−0.0033 (13)	0.0031 (12)	0.0023 (13)
C11_2	0.0291 (17)	0.0358 (18)	0.0239 (15)	−0.0030 (13)	0.0039 (12)	−0.0022 (13)
C12_2	0.0239 (15)	0.0312 (17)	0.0251 (16)	0.0036 (13)	−0.0009 (12)	0.0012 (13)
C13_2	0.0308 (17)	0.0297 (17)	0.0230 (15)	−0.0026 (13)	−0.0002 (12)	0.0017 (13)
C14_2	0.0280 (16)	0.0330 (17)	0.0221 (15)	−0.0048 (13)	0.0051 (12)	0.0015 (13)
C15_2	0.0274 (17)	0.0319 (17)	0.0288 (16)	0.0000 (13)	−0.0001 (13)	−0.0015 (13)
C16_2	0.0312 (18)	0.0289 (16)	0.0321 (17)	−0.0002 (14)	0.0017 (13)	−0.0020 (14)
C17_2	0.041 (2)	0.039 (2)	0.039 (2)	−0.0019 (16)	−0.0103 (16)	−0.0053 (16)

Geometric parameters (Å, º)

S1_1—O1_1	1.468 (2)	S1_2—O1_2	1.470 (2)
S1_1—N2_1	1.747 (3)	S1_2—N2_2	1.744 (3)
S1_1—C7A_1	1.810 (3)	S1_2—C7A_2	1.815 (3)

F1_1—C8_1	1.302 (4)	F1_2—C8_2	1.327 (4)
F2_1—C8_1	1.293 (5)	F2_2—C8_2	1.315 (4)
F3_1—C8_1	1.349 (5)	F3_2—C8_2	1.329 (4)
O2_1—C3_1	1.204 (4)	O2_2—C3_2	1.206 (4)
O3_1—N3_1	1.226 (4)	O3_2—N3_2	1.229 (4)
O4_1—N3_1	1.223 (4)	O4_2—N3_2	1.221 (4)
O5_1—C9_1	1.221 (4)	O5_2—C9_2	1.220 (4)
O6_1—C12_1	1.432 (4)	O6_2—C12_2	1.424 (4)
O6_1—C15_1	1.434 (4)	O6_2—C15_2	1.438 (4)
O7_1—C12_1	1.415 (4)	O7_2—C12_2	1.411 (4)
O7_1—C16_1	1.419 (5)	O7_2—C16_2	1.431 (4)
N2_1—C3_1	1.397 (4)	N2_2—C3_2	1.393 (4)
N2_1—C9_1	1.440 (4)	N2_2—C9_2	1.442 (4)
N3_1—C7_1	1.466 (5)	N3_2—C7_2	1.466 (5)
N4_1—C9_1	1.326 (5)	N4_2—C9_2	1.333 (4)
N4_1—C10_1	1.470 (4)	N4_2—C10_2	1.470 (4)
N4_1—C14_1	1.470 (4)	N4_2—C14_2	1.471 (4)
C3_1—C3A_1	1.488 (4)	C3_2—C3A_2	1.484 (4)
C3A_1—C7A_1	1.375 (5)	C3A_2—C7A_2	1.384 (5)
C3A_1—C4_1	1.391 (5)	C3A_2—C4_2	1.386 (5)
C4_1—C5_1	1.398 (4)	C4_2—C5_2	1.392 (4)
C4_1—H4_1	0.9500	C4_2—H4_2	0.9500
C5_1—C6_1	1.392 (5)	C5_2—C6_2	1.389 (5)
C5_1—C8_1	1.505 (5)	C5_2—C8_2	1.507 (4)
C6_1—C7_1	1.383 (5)	C6_2—C7_2	1.383 (5)
C6_1—H6_1	0.9500	C6_2—H6_2	0.9500
C7_1—C7A_1	1.381 (5)	C7_2—C7A_2	1.374 (5)
C10_1—C11_1	1.517 (5)	C10_2—C11_2	1.532 (5)
C10_1—H10A_1	0.9900	C10_2—H10C_2	0.9900
C10_1—H10B_1	0.9900	C10_2—H10D_2	0.9900
C11_1—C12_1	1.515 (5)	C11_2—C12_2	1.515 (5)
C11_1—H11A_1	0.9900	C11_2—H11C_2	0.9900
C11_1—H11B_1	0.9900	C11_2—H11D_2	0.9900
C12_1—C13_1	1.529 (5)	C12_2—C13_2	1.529 (4)
C13_1—C14_1	1.514 (5)	C13_2—C14_2	1.513 (5)
C13_1—H13A_1	0.9900	C13_2—H13C_2	0.9900
C13_1—H13B_1	0.9900	C13_2—H13D_2	0.9900
C14_1—H14A_1	0.9900	C14_2—H14C_2	0.9900
C14_1—H14B_1	0.9900	C14_2—H14D_2	0.9900
C15_1—C17_1	1.507 (6)	C15_2—C17_2	1.511 (5)
C15_1—C16_1	1.517 (6)	C15_2—C16_2	1.540 (5)
C15_1—H15_1	1.0000	C15_2—H15B_2	1.0000
C16_1—H16A_1	0.9900	C16_2—H16C_2	0.9900
C16_1—H16B_1	0.9900	C16_2—H16D_2	0.9900
C17_1—H17A_1	0.9800	C17_2—H17D_2	0.9800
C17_1—H17B_1	0.9800	C17_2—H17E_2	0.9800
C17_1—H17C_1	0.9800	C17_2—H17F_2	0.9800

O1_1—S1_1—N2_1	105.13 (14)	O1_2—S1_2—N2_2	105.61 (14)
O1_1—S1_1—C7A_1	107.49 (14)	O1_2—S1_2—C7A_2	107.10 (14)
N2_1—S1_1—C7A_1	87.31 (14)	N2_2—S1_2—C7A_2	87.17 (14)
C12_1—O6_1—C15_1	108.7 (3)	C12_2—O6_2—C15_2	105.3 (2)
C12_1—O7_1—C16_1	106.6 (3)	C12_2—O7_2—C16_2	106.7 (2)
C3_1—N2_1—C9_1	126.8 (3)	C3_2—N2_2—C9_2	125.4 (3)
C3_1—N2_1—S1_1	117.7 (2)	C3_2—N2_2—S1_2	118.0 (2)
C9_1—N2_1—S1_1	112.9 (2)	C9_2—N2_2—S1_2	113.8 (2)
O4_1—N3_1—O3_1	124.5 (3)	O4_2—N3_2—O3_2	124.6 (3)
O4_1—N3_1—C7_1	118.5 (3)	O4_2—N3_2—C7_2	118.6 (3)
O3_1—N3_1—C7_1	117.1 (3)	O3_2—N3_2—C7_2	116.8 (3)
C9_1—N4_1—C10_1	117.9 (3)	C9_2—N4_2—C10_2	118.8 (3)
C9_1—N4_1—C14_1	126.5 (3)	C9_2—N4_2—C14_2	126.7 (3)
C10_1—N4_1—C14_1	113.5 (3)	C10_2—N4_2—C14_2	113.5 (3)
O2_1—C3_1—N2_1	125.5 (3)	O2_2—C3_2—N2_2	125.8 (3)
O2_1—C3_1—C3A_1	126.8 (3)	O2_2—C3_2—C3A_2	126.5 (3)
N2_1—C3_1—C3A_1	107.7 (3)	N2_2—C3_2—C3A_2	107.7 (3)
C7A_1—C3A_1—C4_1	121.8 (3)	C7A_2—C3A_2—C4_2	121.6 (3)
C7A_1—C3A_1—C3_1	112.9 (3)	C7A_2—C3A_2—C3_2	112.7 (3)
C4_1—C3A_1—C3_1	125.2 (3)	C4_2—C3A_2—C3_2	125.7 (3)
C3A_1—C4_1—C5_1	117.8 (3)	C3A_2—C4_2—C5_2	117.9 (3)
C3A_1—C4_1—H4_1	121.1	C3A_2—C4_2—H4_2	121.1
C5_1—C4_1—H4_1	121.1	C5_2—C4_2—H4_2	121.1
C6_1—C5_1—C4_1	120.9 (3)	C6_2—C5_2—C4_2	121.2 (3)
C6_1—C5_1—C8_1	119.1 (3)	C6_2—C5_2—C8_2	118.9 (3)
C4_1—C5_1—C8_1	120.0 (3)	C4_2—C5_2—C8_2	119.8 (3)
C7_1—C6_1—C5_1	119.3 (3)	C7_2—C6_2—C5_2	119.1 (3)
C7_1—C6_1—H6_1	120.3	C7_2—C6_2—H6_2	120.5
C5_1—C6_1—H6_1	120.3	C5_2—C6_2—H6_2	120.5
C7A_1—C7_1—C6_1	120.6 (3)	C7A_2—C7_2—C6_2	120.9 (3)
C7A_1—C7_1—N3_1	120.3 (3)	C7A_2—C7_2—N3_2	120.6 (3)
C6_1—C7_1—N3_1	119.1 (3)	C6_2—C7_2—N3_2	118.5 (3)
C3A_1—C7A_1—C7_1	119.4 (3)	C7_2—C7A_2—C3A_2	119.2 (3)
C3A_1—C7A_1—S1_1	113.6 (2)	C7_2—C7A_2—S1_2	127.5 (3)
C7_1—C7A_1—S1_1	126.9 (3)	C3A_2—C7A_2—S1_2	113.3 (2)
F2_1—C8_1—F1_1	109.6 (3)	F2_2—C8_2—F1_2	107.2 (3)
F2_1—C8_1—F3_1	104.7 (3)	F2_2—C8_2—F3_2	107.2 (3)
F1_1—C8_1—F3_1	105.5 (3)	F1_2—C8_2—F3_2	106.2 (3)
F2_1—C8_1—C5_1	113.5 (3)	F2_2—C8_2—C5_2	113.0 (3)
F1_1—C8_1—C5_1	112.6 (3)	F1_2—C8_2—C5_2	111.2 (3)
F3_1—C8_1—C5_1	110.3 (3)	F3_2—C8_2—C5_2	111.7 (3)
O5_1—C9_1—N4_1	125.8 (3)	O5_2—C9_2—N4_2	126.3 (3)
O5_1—C9_1—N2_1	117.8 (3)	O5_2—C9_2—N2_2	118.6 (3)
N4_1—C9_1—N2_1	116.5 (3)	N4_2—C9_2—N2_2	115.1 (3)
N4_1—C10_1—C11_1	110.5 (3)	N4_2—C10_2—C11_2	109.7 (3)
N4_1—C10_1—H10A_1	109.5	N4_2—C10_2—H10C_2	109.7
C11_1—C10_1—H10A_1	109.5	C11_2—C10_2—H10C_2	109.7
N4_1—C10_1—H10B_1	109.5	N4_2—C10_2—H10D_2	109.7

C11_1—C10_1—H10B_1	109.5	C11_2—C10_2—H10D_2	109.7
H10A_1—C10_1—H10B_1	108.1	H10C_2—C10_2—H10D_2	108.2
C12_1—C11_1—C10_1	110.6 (3)	C12_2—C11_2—C10_2	111.0 (3)
C12_1—C11_1—H11A_1	109.5	C12_2—C11_2—H11C_2	109.4
C10_1—C11_1—H11A_1	109.5	C10_2—C11_2—H11C_2	109.4
C12_1—C11_1—H11B_1	109.5	C12_2—C11_2—H11D_2	109.4
C10_1—C11_1—H11B_1	109.5	C10_2—C11_2—H11D_2	109.4
H11A_1—C11_1—H11B_1	108.1	H11C_2—C11_2—H11D_2	108.0
O7_1—C12_1—O6_1	106.8 (3)	O7_2—C12_2—O6_2	105.6 (3)
O7_1—C12_1—C11_1	109.5 (3)	O7_2—C12_2—C11_2	110.0 (3)
O6_1—C12_1—C11_1	109.9 (3)	O6_2—C12_2—C11_2	108.5 (3)
O7_1—C12_1—C13_1	111.6 (3)	O7_2—C12_2—C13_2	111.5 (3)
O6_1—C12_1—C13_1	108.1 (3)	O6_2—C12_2—C13_2	111.0 (3)
C11_1—C12_1—C13_1	110.8 (3)	C11_2—C12_2—C13_2	110.1 (3)
C14_1—C13_1—C12_1	109.6 (3)	C14_2—C13_2—C12_2	109.8 (3)
C14_1—C13_1—H13A_1	109.8	C14_2—C13_2—H13C_2	109.7
C12_1—C13_1—H13A_1	109.8	C12_2—C13_2—H13C_2	109.7
C14_1—C13_1—H13B_1	109.8	C14_2—C13_2—H13D_2	109.7
C12_1—C13_1—H13B_1	109.8	C12_2—C13_2—H13D_2	109.7
H13A_1—C13_1—H13B_1	108.2	H13C_2—C13_2—H13D_2	108.2
N4_1—C14_1—C13_1	110.8 (3)	N4_2—C14_2—C13_2	110.7 (3)
N4_1—C14_1—H14A_1	109.5	N4_2—C14_2—H14C_2	109.5
C13_1—C14_1—H14A_1	109.5	C13_2—C14_2—H14C_2	109.5
N4_1—C14_1—H14B_1	109.5	N4_2—C14_2—H14D_2	109.5
C13_1—C14_1—H14B_1	109.5	C13_2—C14_2—H14D_2	109.5
H14A_1—C14_1—H14B_1	108.1	H14C_2—C14_2—H14D_2	108.1
O6_1—C15_1—C17_1	109.7 (3)	O6_2—C15_2—C17_2	108.8 (3)
O6_1—C15_1—C16_1	101.4 (3)	O6_2—C15_2—C16_2	103.1 (3)
C17_1—C15_1—C16_1	115.3 (3)	C17_2—C15_2—C16_2	115.1 (3)
O6_1—C15_1—H15_1	110.0	O6_2—C15_2—H15B_2	109.9
C17_1—C15_1—H15_1	110.0	C17_2—C15_2—H15B_2	109.9
C16_1—C15_1—H15_1	110.0	C16_2—C15_2—H15B_2	109.9
O7_1—C16_1—C15_1	103.3 (3)	O7_2—C16_2—C15_2	105.4 (3)
O7_1—C16_1—H16A_1	111.1	O7_2—C16_2—H16C_2	110.7
C15_1—C16_1—H16A_1	111.1	C15_2—C16_2—H16C_2	110.7
O7_1—C16_1—H16B_1	111.1	O7_2—C16_2—H16D_2	110.7
C15_1—C16_1—H16B_1	111.1	C15_2—C16_2—H16D_2	110.7
H16A_1—C16_1—H16B_1	109.1	H16C_2—C16_2—H16D_2	108.8
C15_1—C17_1—H17A_1	109.5	C15_2—C17_2—H17D_2	109.5
C15_1—C17_1—H17B_1	109.5	C15_2—C17_2—H17E_2	109.5
H17A_1—C17_1—H17B_1	109.5	H17D_2—C17_2—H17E_2	109.5
C15_1—C17_1—H17C_1	109.5	C15_2—C17_2—H17F_2	109.5
H17A_1—C17_1—H17C_1	109.5	H17D_2—C17_2—H17F_2	109.5
H17B_1—C17_1—H17C_1	109.5	H17E_2—C17_2—H17F_2	109.5
O1_1—S1_1—N2_1—C3_1	113.0 (2)	O1_2—S1_2—N2_2—C3_2	−114.6 (2)
C7A_1—S1_1—N2_1—C3_1	5.6 (3)	C7A_2—S1_2—N2_2—C3_2	−7.6 (2)
O1_1—S1_1—N2_1—C9_1	−84.0 (2)	O1_2—S1_2—N2_2—C9_2	83.3 (2)

C7A_1—S1_1—N2_1—C9_1	168.6 (2)	C7A_2—S1_2—N2_2—C9_2	−169.7 (2)
C9_1—N2_1—C3_1—O2_1	8.8 (6)	C9_2—N2_2—C3_2—O2_2	−6.6 (5)
S1_1—N2_1—C3_1—O2_1	169.0 (3)	S1_2—N2_2—C3_2—O2_2	−166.4 (3)
C9_1—N2_1—C3_1—C3A_1	−169.5 (3)	C9_2—N2_2—C3_2—C3A_2	171.4 (3)
S1_1—N2_1—C3_1—C3A_1	−9.2 (3)	S1_2—N2_2—C3_2—C3A_2	11.6 (3)
O2_1—C3_1—C3A_1—C7A_1	−169.4 (3)	O2_2—C3_2—C3A_2—C7A_2	167.7 (3)
N2_1—C3_1—C3A_1—C7A_1	8.9 (4)	N2_2—C3_2—C3A_2—C7A_2	−10.3 (4)
O2_1—C3_1—C3A_1—C4_1	8.9 (6)	O2_2—C3_2—C3A_2—C4_2	−11.0 (5)
N2_1—C3_1—C3A_1—C4_1	−172.9 (3)	N2_2—C3_2—C3A_2—C4_2	170.9 (3)
C7A_1—C3A_1—C4_1—C5_1	2.3 (5)	C7A_2—C3A_2—C4_2—C5_2	−2.5 (5)
C3_1—C3A_1—C4_1—C5_1	−175.8 (3)	C3_2—C3A_2—C4_2—C5_2	176.1 (3)
C3A_1—C4_1—C5_1—C6_1	−0.4 (5)	C3A_2—C4_2—C5_2—C6_2	1.1 (5)
C3A_1—C4_1—C5_1—C8_1	178.0 (3)	C3A_2—C4_2—C5_2—C8_2	−176.4 (3)
C4_1—C5_1—C6_1—C7_1	−1.0 (5)	C4_2—C5_2—C6_2—C7_2	0.1 (5)
C8_1—C5_1—C6_1—C7_1	−179.3 (3)	C8_2—C5_2—C6_2—C7_2	177.6 (3)
C5_1—C6_1—C7_1—C7A_1	0.5 (5)	C5_2—C6_2—C7_2—C7A_2	0.1 (4)
C5_1—C6_1—C7_1—N3_1	−179.6 (3)	C5_2—C6_2—C7_2—N3_2	−179.8 (3)
O4_1—N3_1—C7_1—C7A_1	−173.3 (3)	O4_2—N3_2—C7_2—C7A_2	169.6 (3)
O3_1—N3_1—C7_1—C7A_1	7.5 (5)	O3_2—N3_2—C7_2—C7A_2	−11.4 (4)
O4_1—N3_1—C7_1—C6_1	6.8 (4)	O4_2—N3_2—C7_2—C6_2	−10.5 (4)
O3_1—N3_1—C7_1—C6_1	−172.5 (3)	O3_2—N3_2—C7_2—C6_2	168.5 (3)
C4_1—C3A_1—C7A_1—C7_1	−2.8 (5)	C6_2—C7_2—C7A_2—C3A_2	−1.5 (4)
C3_1—C3A_1—C7A_1—C7_1	175.5 (3)	N3_2—C7_2—C7A_2—C3A_2	178.4 (3)
C4_1—C3A_1—C7A_1—S1_1	176.5 (2)	C6_2—C7_2—C7A_2—S1_2	176.9 (2)
C3_1—C3A_1—C7A_1—S1_1	−5.2 (3)	N3_2—C7_2—C7A_2—S1_2	−3.2 (4)
C6_1—C7_1—C7A_1—C3A_1	1.4 (4)	C4_2—C3A_2—C7A_2—C7_2	2.7 (5)
N3_1—C7_1—C7A_1—C3A_1	−178.6 (3)	C3_2—C3A_2—C7A_2—C7_2	−176.1 (3)
C6_1—C7_1—C7A_1—S1_1	−177.8 (2)	C4_2—C3A_2—C7A_2—S1_2	−175.9 (2)
N3_1—C7_1—C7A_1—S1_1	2.2 (4)	C3_2—C3A_2—C7A_2—S1_2	5.3 (3)
O1_1—S1_1—C7A_1—C3A_1	−104.9 (2)	O1_2—S1_2—C7A_2—C7_2	−72.1 (3)
N2_1—S1_1—C7A_1—C3A_1	0.1 (2)	N2_2—S1_2—C7A_2—C7_2	−177.6 (3)
O1_1—S1_1—C7A_1—C7_1	74.3 (3)	O1_2—S1_2—C7A_2—C3A_2	106.3 (2)
N2_1—S1_1—C7A_1—C7_1	179.3 (3)	N2_2—S1_2—C7A_2—C3A_2	0.9 (2)
C6_1—C5_1—C8_1—F2_1	−157.6 (3)	C6_2—C5_2—C8_2—F2_2	157.3 (3)
C4_1—C5_1—C8_1—F2_1	24.0 (5)	C4_2—C5_2—C8_2—F2_2	−25.1 (4)
C6_1—C5_1—C8_1—F1_1	77.1 (4)	C6_2—C5_2—C8_2—F1_2	−82.1 (4)
C4_1—C5_1—C8_1—F1_1	−101.3 (4)	C4_2—C5_2—C8_2—F1_2	95.5 (4)
C6_1—C5_1—C8_1—F3_1	−40.4 (4)	C6_2—C5_2—C8_2—F3_2	36.4 (4)
C4_1—C5_1—C8_1—F3_1	141.2 (3)	C4_2—C5_2—C8_2—F3_2	−146.1 (3)
C10_1—N4_1—C9_1—O5_1	−2.5 (5)	C10_2—N4_2—C9_2—O5_2	5.0 (5)
C14_1—N4_1—C9_1—O5_1	159.9 (3)	C14_2—N4_2—C9_2—O5_2	−162.5 (3)
C10_1—N4_1—C9_1—N2_1	179.8 (3)	C10_2—N4_2—C9_2—N2_2	−176.4 (3)
C14_1—N4_1—C9_1—N2_1	−17.8 (5)	C14_2—N4_2—C9_2—N2_2	16.1 (4)
C3_1—N2_1—C9_1—O5_1	127.2 (4)	C3_2—N2_2—C9_2—O5_2	−125.1 (3)
S1_1—N2_1—C9_1—O5_1	−33.9 (4)	S1_2—N2_2—C9_2—O5_2	35.4 (4)
C3_1—N2_1—C9_1—N4_1	−54.9 (4)	C3_2—N2_2—C9_2—N4_2	56.2 (4)
S1_1—N2_1—C9_1—N4_1	144.0 (2)	S1_2—N2_2—C9_2—N4_2	−143.3 (2)
C9_1—N4_1—C10_1—C11_1	−138.9 (3)	C9_2—N4_2—C10_2—C11_2	134.3 (3)

C14_1—N4_1—C10_1—C11_1	56.4 (4)	C14_2—N4_2—C10_2—C11_2	−56.6 (4)
N4_1—C10_1—C11_1—C12_1	−55.0 (4)	N4_2—C10_2—C11_2—C12_2	55.3 (4)
C16_1—O7_1—C12_1—O6_1	19.5 (4)	C16_2—O7_2—C12_2—O6_2	−32.4 (3)
C16_1—O7_1—C12_1—C11_1	138.5 (3)	C16_2—O7_2—C12_2—C11_2	−149.2 (3)
C16_1—O7_1—C12_1—C13_1	−98.5 (3)	C16_2—O7_2—C12_2—C13_2	88.3 (3)
C15_1—O6_1—C12_1—O7_1	4.1 (4)	C15_2—O6_2—C12_2—O7_2	38.7 (3)
C15_1—O6_1—C12_1—C11_1	−114.7 (3)	C15_2—O6_2—C12_2—C11_2	156.5 (3)
C15_1—O6_1—C12_1—C13_1	124.3 (3)	C15_2—O6_2—C12_2—C13_2	−82.3 (3)
C10_1—C11_1—C12_1—O7_1	179.5 (3)	C10_2—C11_2—C12_2—O7_2	−179.5 (3)
C10_1—C11_1—C12_1—O6_1	−63.5 (4)	C10_2—C11_2—C12_2—O6_2	65.5 (3)
C10_1—C11_1—C12_1—C13_1	56.0 (4)	C10_2—C11_2—C12_2—C13_2	−56.1 (4)
O7_1—C12_1—C13_1—C14_1	−178.6 (3)	O7_2—C12_2—C13_2—C14_2	178.9 (3)
O6_1—C12_1—C13_1—C14_1	64.2 (4)	O6_2—C12_2—C13_2—C14_2	−63.6 (4)
C11_1—C12_1—C13_1—C14_1	−56.3 (4)	C11_2—C12_2—C13_2—C14_2	56.5 (3)
C9_1—N4_1—C14_1—C13_1	139.5 (3)	C9_2—N4_2—C14_2—C13_2	−133.8 (3)
C10_1—N4_1—C14_1—C13_1	−57.5 (4)	C10_2—N4_2—C14_2—C13_2	58.2 (4)
C12_1—C13_1—C14_1—N4_1	56.0 (4)	C12_2—C13_2—C14_2—N4_2	−56.7 (3)
C12_1—O6_1—C15_1—C17_1	−146.3 (3)	C12_2—O6_2—C15_2—C17_2	−151.2 (3)
C12_1—O6_1—C15_1—C16_1	−23.9 (4)	C12_2—O6_2—C15_2—C16_2	−28.6 (3)
C12_1—O7_1—C16_1—C15_1	−34.1 (4)	C12_2—O7_2—C16_2—C15_2	13.8 (3)
O6_1—C15_1—C16_1—O7_1	35.2 (4)	O6_2—C15_2—C16_2—O7_2	9.2 (3)
C17_1—C15_1—C16_1—O7_1	153.6 (3)	C17_2—C15_2—C16_2—O7_2	127.5 (3)